Journal of Imaging Science and Technology® 59(2): 020504-1–020504-9, 2015.

Preferred Racial Skin Color Reproduction in an Image based on Race Classification

Dae-Chul Kim▲, Wang-Jun Kyung▲, and Yeong-Ho Ha▲
School of Electronics Engineering, Kyungpook National University, 80 Daehakro, Bukgu, Daegu 702-701, Korea
E-mail: yha@ee.knu.ac.kr

Abstract. *Preferred skin color reproduction is an important factor for improving the image quality of display devices and systems. Therefore, this article presents a race-selective preferred skin color reproduction method for the case of multiple races in a single image. First, the proposed method detects skin regions using a focus map and skin candidate map. Next, the race of each detected skin region is classified by comparing the Euclidean distance of the average chromaticity for each detected skin region with a database of racial skin colors. Based on this classification, the racial preferred skin color for each detected skin region is then selected from candidate racial preferred skin colors that are predefined in a database generated through an observer's preference test. Finally, the skin color is reproduced toward the preferred skin color. Experimental results confirm that the proposed method can achieve race-selective preferred skin color reproduction in the case of multiple races in a single image.* © *2015 Society for Imaging Science and Technology.*
[DOI: 10.2352/J.ImagingSci.Technol.2015.59.2.020504]

INTRODUCTION

Preference colors are typically determined according to the observer's preference, and are an important subjective measure for image quality evaluation of display equipment. The preference indicates the degree of satisfaction of the observer and is generally enhanced by reproducing the colors of sky, grass, and skin.[1] Among these colors, skin color is one of the main factors in preferred color reproduction, as humans tend to perceive people before anything else in an image based on recognizing the skin color.[2,3] Therefore, the skin color needs to be enhanced to become more natural for the viewer.

Various skin color reproduction methods have already been studied. Kao proposed color reproduction using a color transformation matrix.[4] Sanger modeled the preferred skin color area using an ellipse and proposed three preferred skin color ellipses according to the ethnic groups of Asian, Caucasian, and African.[2] Yendrikhovskij proposed the enhancement of perceived naturalness using a comparison between reproduced color and preference colors.[5] Kim proposed mapping toward the preferred skin color region using an affine transform.[6] Nachlieli proposed sensitive skin color enhancement to correspond to human preferences regarding the appearance of people based on CIELab color space.[7] However, all of these studies focus on mapping the skin colors of different races to a single skin color, which is mapped to the mean value of preferred skin colors.

Accordingly, this article proposes race-selective preferred skin color reproduction to consider multiple races in a single image. First, two databases are generated: a database of racial skin colors to classify races and a database of candidate racial preferred skin colors to select the preferred skin color for each detected skin region. As shown in Figure 1, the proposed method first detects a skin region using a focus map and skin candidate map. Next, the race of the detected skin region is classified by calculating the Euclidean distance between the average chromaticity of the skin region and the chromaticity of each racial skin color from the database. The preferred skin color for each classified racial skin region is then selected using the Euclidean distance from the database of candidate racial preferred skin colors. Finally, the skin color in each detected skin region is reproduced toward each preferred skin color. Experimental results show that the proposed method can achieve preferred skin color reproduction for multiple races in an image.

GENERATION OF DATABASE OF RACIAL SKIN COLORS AND CANDIDATE RACIAL PREFERRED SKIN COLORS

The proposed method uses two predefined databases: a database of racial skin colors and a database of candidate racial preferred skin colors, where the former is used for race classification and the latter for the selection of the racial preferred skin color.

Generation of Database of Racial Skin Colors

The chromaticity distribution and luminance distribution of each racial skin color are important information. First, 200 images of each race are selected from magazine websites and their skin regions are manually obtained using an image editing tool. All the pixels in the skin regions for each race are then converted to YCbCr color space to calculate the luminance and chrominance. Next, as shown in Tables I and II, the distribution of pixels in the skin regions and average chromaticity for each luminance level, ranging from 0 to 1 in steps of 0.1, are calculated. The former determines the distribution of racial skin colors for each luminance level and is used as a weighting factor in race classification. Meanwhile, the latter determines the chromaticities of the racial skin

▲ IS&T Members.

Received Mar. 4, 2014; accepted for publication Apr. 22, 2015; published online May 28, 2015. Associate Editor: Susan Farnand.
1062-3701/2015/59(2)/020504/9/$25.00

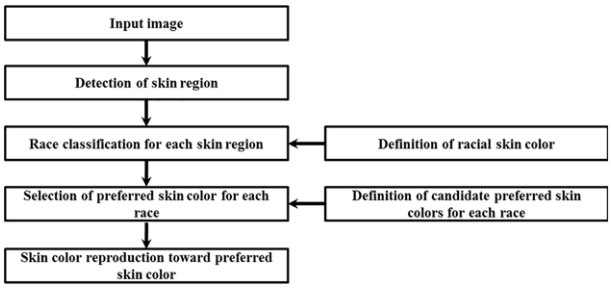

Figure 1. Block diagram of the proposed skin color reproduction.

Table I. Distribution percentage of skin pixels in the skin regions for each race per luminance level.

Luminance level	Asian		African		Caucasian	
	Pixels	Distribution	Pixels	Distribution	Pixels	Distribution
0	151	0	71,304	0.02	2	0
0.1	5223	0	449,598	0.15	131	0
0.2	69,243	0.02	661,414	0.22	7868	0
0.3	266,287	0.07	577,579	0.19	113,503	0.03
0.4	507,126	0.14	483,881	0.16	335,451	0.09
0.5	689,717	0.19	332,433	0.11	572,819	0.16
0.6	734,355	0.2	196,735	0.06	687,160	0.19
0.7	652,555	0.18	108,303	0.04	722,907	0.2
0.8	381,624	0.11	69,609	0.02	613,556	0.17
0.9	201,873	0.06	48,243	0.02	388,748	0.11
1	83,586	0.02	52,608	0.02	147,399	0.04

Table II. Average chromaticity of racial skin colors per luminance level.

Luminance level	Asian		African		Caucasian	
	Cb	Cr	Cb	Cr	Cb	Cr
0	126	132	125	132	124	135
0.1	119	140	122	137	119	143
0.2	112	145	120	140	113	150
0.3	107	152	117	145	111	151
0.4	101	155	111	150	108	154
0.5	99	155	111	151	108	154
0.6	99	154	111	150	106	156
0.7	101	152	114	145	111	149
0.8	106	146	121	138	116	142
0.9	116	138	126	131	116	140
1	126	129	127	128	127	129

colors for each luminance level and is used to generate the database of racial skin colors. Finally, a database for each racial skin color is generated by collecting three racial skin colors for each luminance level for Asians, Caucasians, and Africans.

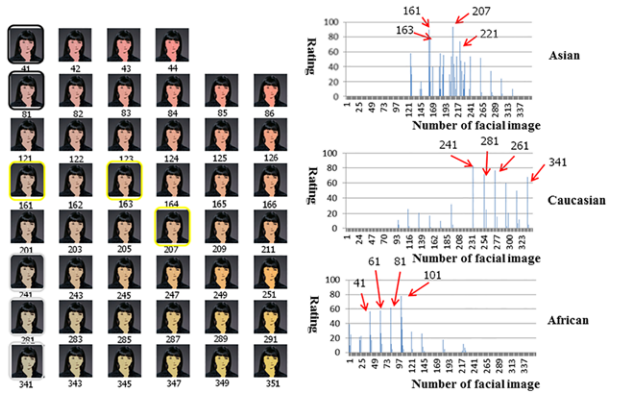

Figure 2. Samples of facial images and scores of facial images: (a) the samples of 360 facial images at the luminance level of 0.7, (b) the scores of facial images at the luminance level of 0.7.

Generation of Database of Candidate Racial Preferred Skin Colors

The database of candidate racial preferred skin colors is necessary to select the preferred skin color in a detected skin region for each classified race of Asian, Caucasian, and African, and is based on an observer's preference test. For Asians, 360 prototype skin images are generated by changing the hue and saturation values under a predefined skin color based on HSV color space. The range of hue for skin color is taken between 0 and 51 in steps of 3 and the range of saturation for skin color is taken between 0.12 and 0.7 in steps of 0.03; a total of 360 skin images can be generated by keeping luminance constant. Subsequently, 11 pairs of 360 prototype skin images are generated with luminance varied from 0 to 1 in steps of 0.1. Therefore, a total of 360 × 11 prototype skin images are generated with various hue, saturation, and luminance values.

Next, each pair of 360 prototype skin images is printed and evaluated by the observer. Each observer selects 30% of the images from the prototype skin images with a constant luminance value and grades the selected images from 1 to 5. Figure 2(a) shows the 360 prototype skin images under a luminance level of 0.7 and Fig. 2(b) shows their respective scores. This preference test is repeated for all 11 pairs of prototype skin images by 100 observers, who include 45 females and 55 males aged between 20 and 34. This evaluation experiment is conducted using a Macbeth Judge II-S viewing booth, which supports a standard illuminant (D65) with 750 lx. This same preference test is also repeated for the other races, i.e., Caucasian and African. Fig. 2(b) represents the number of preferred prototype skin images for Asian, Caucasian, and African races.

The evaluation test by itself did not produce one preferred skin color, as several skin images received high scores. Therefore, for each luminance level, four candidate preferred skin images with over half of the total scores were selected for each race. Each preference rate R_p was then calculated using the ratio of the earned score E_p to the total

Table III. Selected racial preferred skin colors using an observer's preference test at a luminance level of 0.7.

	Cb	Cr	Score E_p	Total score E_{max}	Preference rate R_p
Asian	103	153	724	1380	52.4%
	112	148	711	1380	51.5%
	95	155	697	1380	50.5%
	90	158	694	1380	50.2%
African	103	150	751	1380	54.4%
	117	142	726	1380	52.6%
	121	137	712	1380	51.6%
	80	165	709	1380	51.3%
Caucasian	108	152	779	1380	56.4%
	112	153	766	1380	55.5%
	103	155	754	1380	54.6%

score $E_{\max}$ as follows:

$$R_p = 1 + \left(1 - \frac{E_p}{E_{\max}}\right), \tag{1}$$

where subscript p represents the four candidate preferred skin colors, which were then used as the weighting factor to select the preferred skin color in a detected skin region.

Next, In order to reduce the complexity in measuring the chromaticity of selected skin images, we used a patch of dimensions 1 cm × 1 cm for each selected skin color. Then, these color patches were each measured using a GretagMacbeth Spectrolino with a D65 filter to obtain the tri-stimulus values (CIEXYZ) of the candidate preferred skin colors. A YCbCr conversion of the measured data was then performed to reproduce the skin color for each luminance level.

Table III shows the chromaticities of the four candidates for the preferred skin color for each race and the preference rates under a luminance level of 0.7. Finally, a database of the candidate racial preferred skin colors was generated by collecting the chromaticities of the four candidate preferred skin colors and preference rates for each luminance level for Asian, Caucasian, and African, which was then used to select the preferred skin color in a detected skin region.

DETECTION OF SKIN REGIONS

Skin color detection is generally performed using skin color models of various color spaces. Most previous research on skin region detection based on skin color was performed in the RGB, YCbCr, and HSV color spaces.[8–10] However, these skin region detection methods produce different results due to different skin color distributions in each color space.

Therefore, to improve the skin color detection accuracy, a skin color detection method is proposed that combines a skin candidate map and focus map. The skin detection rates of the skin color models for the RGB, YCbCr, and HSV color spaces are first calculated. A skin candidate map considering the detection rates and focus map is then generated. Finally, skin regions are detected by selecting the common regions between the skin candidate map and the focus map.

Calculation of Skin Detection Rates

To calculate the skin detection rates of the skin color models for the RGB, YCbCr, and HSV color spaces, 100 images of each race are selected from websites and their skin regions are manually extracted using an image editing tool to obtain reference skin regions. The skin detection is then performed using each predefined skin color threshold from the RGB, YCbCr, and HSV color spaces. Next, the TP (true positive) and FP (false positive) are calculated to obtain the detection rate of each color space.[11] The TP and FP are calculated based on the detected pixels inside and outside the reference skin regions. The TP is obtained using the ratio of the detected pixels to all the pixels in the skin regions while the FP is obtained using the ratio of the detected pixels to all the pixels outside the skin regions as follows:

$$\mathrm{TP} = \frac{N_{\mathrm{TP}}}{N_I}, \tag{2}$$

$$\mathrm{FP} = \frac{N_{\mathrm{FP}}}{N_O}, \tag{3}$$

where N_{TP} is the number of detected pixels and N_I is the number of all the pixels in the skin regions, whereas N_{FP} is the number of detected pixels and N_O is the number of all the pixels outside the skin regions. The detection rate of each skin color model, w_t, is then calculated using the ratio of TP to FP for each skin color model:

$$w_t = \frac{\mathrm{TP}_t}{\mathrm{FP}_t}, \quad t = 1, 2, 3, \tag{4}$$

where the subscript t with value 1, 2, or 3 indicates the RGB, YCbCr, and HSV color spaces, respectively. The detection rates are then used as weighting factors to generate a skin candidate map.

Detection of Skin Regions Using the Skin Candidate Map and Focus Map

This section presents a skin color detection method that combines the skin candidate map and the focus map. First, a skin candidate map, $c(x, y)$, that considers the detection rate w_t is calculated as follows:

$$c(x, y) = \sum_{t=1}^{3} w_t D_t(x, y), \tag{5}$$

where D_t denotes a skin color, and the subscript t with value 1, 2, or 3 indicates the RGB, YCbCr, and HSV color spaces, respectively. The skin candidate map includes all the skin regions identified when using the three color space methods, and the false detection rate decreases when the threshold T_1 is adopted in the skin candidate map. Since w_1, w_2, and w_3 are calculated as 2.83, 2.51, and 2.88, respectively, according to Table IV, the threshold is determined based on satisfying at least two of the three color space methods and is set at 5, between 2.89 and 5.34. The skin candidate map with the

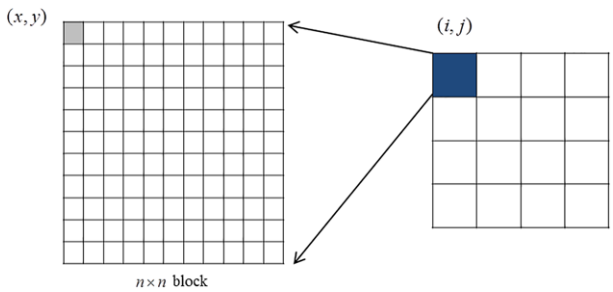

Figure 3. Feature detection process using $n \times n$ blocks: (a) pixels in the divided block, (b) divided blocks of image.

threshold, $c'(x, y)$, is calculated as follows:

$$c'(x,y) = \begin{cases} 1, & c(x,y) \geq T_1, \\ 0, & c(x,y) < T_1. \end{cases} \tag{6}$$

Second, the focus map, $F(i, j)$, is obtained by calculating the gray level variance of each block in Figure 3 as follows:

$$F(i,j) = \frac{1}{N} \sum_{g(x,y) \in U(i,j)} |g(x,y) - \mu_U(i,j)|^2, \tag{7}$$

where N is the number of pixels in each divided block, $g(x, y)$ represents the gray level for the current pixel in a divided block, $U(i, j)$ represents the location of a block in the image, and $\mu_U(i, j)$ is the average gray level for a divided region. To detect a high focus region, the threshold T_2 is then adopted in the focus map and is set at 10, empirically:

$$F(i,j) = \begin{cases} 1, & F(i,j) \geq T_2, \\ 0, & F(i,j) < T_2. \end{cases} \tag{8}$$

However, only boundary blocks of an object are detected when using the gray level variance. Therefore, the focus map is compensated by considering eight neighboring blocks. The number of positive values in the eight neighboring blocks, $V(i, j)$, is calculated as follows:

$$V(i,j) = \sum_{a=-1}^{1} \sum_{b=-1}^{1} F(i+a, j+b). \tag{9}$$

The compensated focus map, $F'(i, j)$, is then determined by filling an empty block when it has over three positive values among the eight neighboring blocks:

$$F'(i,j) = \begin{cases} 1, & \text{if } V(i,j) \geq 3, \\ 0, & \text{otherwise.} \end{cases} \tag{10}$$

Finally, skin regions are determined by selecting common regions between the skin candidate map $c'(i, j)$ and the compensated focus map $F'(i, j)$, giving the results in Figure 4. Panels (a)–(d) in Fig. 4 show the original image, skin candidate map, focus map, and skin detection results, respectively. The skin candidate map has detection errors in the background region, as shown in Fig. 4(b). Also, the focused object was detected from the compensated focus map, as shown in Fig. 4(c). Since a combination of the skin candidate map and the compensated focus map is used for skin color detection, the skin detection error due to false detection of background (Fig. 4(b)) can be avoided in the proposed skin detection result. A comparison of the TP and FP between the proposed and color-space-based methods is presented in Table IV. As shown, the proposed method reduces the false detection rate while improving the detection accuracy.

Table IV. True positive and false positive results using RGB, YCbCr, and HSV color spaces and their comparison with the proposed method.

	RGB	YCbCr	HSV	The proposed method using a 5 × 5 block
Detected pixels from images	1,968,348	1,613,767	1,484,704	1,534,716
Detected pixels from skin regions	1,361,924	1,140,094	1,113,450	1,253,174
Total pixels of skin regions	1,546,399	1,546,399	1,546,399	1,546,399
TP	88%	74%	72%	81%
FP	31%	29%	25%	18%

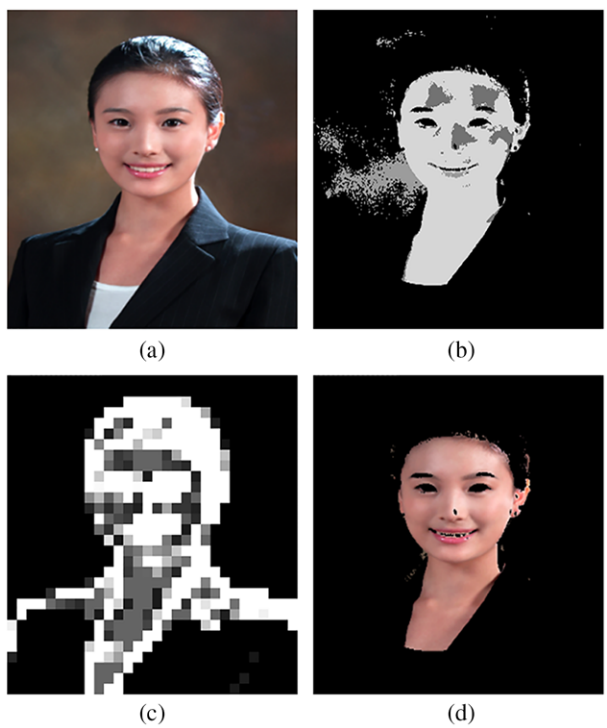

Figure 4. Skin color detection results using the proposed method: (a) original image, (b) skin candidate map, (c) focus map, (d) skin color detected image.

RACE-SELECTIVE PREFERRED SKIN COLOR REPRODUCTION

The proposed method suggests race-selective preferred skin color reproduction for each detected skin region to consider

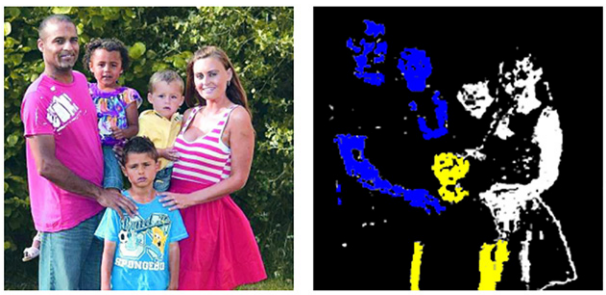

Figure 5. Result of race classification: (a) original image, (b) result of race classification.

the case of a single and multiple races in one image. To correct the preferred skin color according to the race, race classification in each detected skin region is first needed. Then, in each detected skin region, the appropriate preferred skin color is selected. Finally, the skin color in each detected skin region is reproduced toward each appropriate preferred skin color.

Race Classification

Race classification is performed in each detected skin region. In a detected skin region, the average chromaticity and average luminance are first calculated. The average luminance is then categorized in a particular luminance level, ranging from 0 to 1 in steps of 0.1. Thereafter, three chromaticities of racial skin colors and three distributions of racial skin colors are selected from the database of racial skin colors based on the average luminance. To find the color differences between the average chromaticity and the three chromaticities of racial skin colors, referred to as $(\mathrm{Cb}_m, \mathrm{Cr}_m)$ and $(\mathrm{Cb}_{mr}, \mathrm{Cr}_{mr})$, their Euclidean distances, d_r, are calculated by applying the distributions of the racial skin colors, P_r, as a weighting factor:

$$d_r = (1 - P_r)[(\mathrm{Cb}_m - \mathrm{Cb}_{mr})^2 + (\mathrm{Cr}_m - \mathrm{Cr}_{mr})^2]^{1/2}, \quad (11)$$

where r denotes one of three races such as Asian, Caucasian, and African.

Next, the race, S_r, in a detected skin region is classified by selecting the racial color with the minimum Euclidean distance:

$$S_r = \min_r [d_r]. \quad (12)$$

These processes are repeated for all the skin regions. Figure 5 shows the results of the race classification.

Meanwhile, to check the performance validity of the above race classification, a separate experiment with 50 test images for each race was performed. The skin regions were manually extracted and used as the reference skin regions. First, for Caucasian, the skin regions in 50 test images of Caucasians were manually extracted using an image editing tool. Next, the race classification was performed in the skin regions. For Caucasian, the true rate was then calculated using the ratio of the number of Caucasians from the race classification to the number of skin regions. The false rate was calculated using the ratio of the number of Africans and Asians from the race classification to the number of skin regions. This process was repeated for all the test images of the other races and the results are presented in Table V. As shown, the true rate for African was high, whereas the true rates for Asian and Caucasian were found to be mixed together due to similar distributions of the skin chromaticity.

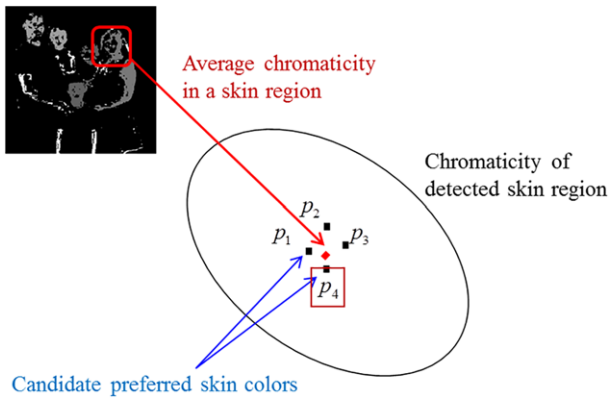

Figure 6. Selection of preferred skin color.

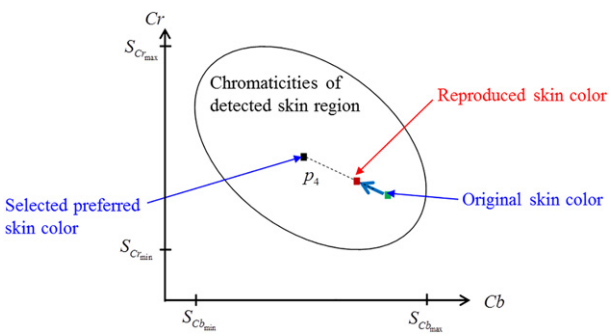

Figure 7. The preferred skin color reproduction toward selected preferred skin color.

Table V. The performance of race classification.

	Skin regions	True	False	True rate
Asian	71	44	27	62%
African	76	59	17	78%
Caucasian	73	42	31	57%

Selection of Preferred Skin Color for Classified Race

Generally, the skin colors for a particular race show certain tendencies, such as reddish or yellowish. Also, the result of the preference test for making the database of candidate racial preferred skin colors did not indicate one preferred skin color, as several skin images received high scores. Thus, to improve the preference of skin color reproduction, the appropriate preferred skin color needs to be selected according to the tendency of the skin color.

However, if the selection of the preferred skin color is performed for all pixels in a detected skin region, this produces artifacts like contouring, as all the pixels in a

Figure 8. Test images including single and multiple races: (a) baby1, (b) child, (c) racing girl, (d) baby2, (e) volunteers, (f) peace corps.

detected skin region are reproduced toward the preferred skin color. Therefore, this article selects an appropriate preferred skin color for each detected skin region. Based on race classification, the average chromaticity and average luminance are obtained for each detected skin region. Then, in a detected skin region, four chromaticities of candidate preferred skin colors for the classified race and their preference rates are selected from a predefined database based on the average luminance. To find the color differences between the average chromaticity and the four chromaticities of the candidate preferred skin colors, respectively referred to as $(\mathrm{Cb}_m, \mathrm{Cr}_m)$ and $(\mathrm{Cb}_p, \mathrm{Cr}_p)$, their Euclidean distances, d_p, are calculated using each preference rate R_p as the weighting factor:

$$d_p = R_p\sqrt{(\mathrm{Cb}_p - \mathrm{Cb}_m)^2 + (\mathrm{Cr}_p - \mathrm{Cr}_m)^2}. \tag{13}$$

The preferred skin color, S_p, is then determined by selecting the candidate preferred skin color with the minimum Euclidean distance:

$$S_p = \min_{p=1,2,3,4}[d_p]. \tag{14}$$

These processes are repeated for all the detected skin regions. As a result, each appropriate preferred skin color is selected in each detected skin region. This process is shown in Figure 6, where the black points indicate the four candidate preferred skin colors for the classified race and the green points indicate the average chromaticity of a detected skin region.

Skin Color Reproduction toward Preferred Skin Color

Once the preferred skin color is selected, the pixels of the original skin color in the detected skin region are mapped toward the preferred skin color.

First, in a detected skin region, the differences between the chromaticities, $(\mathrm{Cb}_i, \mathrm{Cr}_i)$, of the original skin color and the chromaticities, $(\mathrm{Cb}_{S_p}, \mathrm{Cr}_{S_p})$, of the selected preferred skin color for the region are calculated. Then, to avoid color and contouring artifacts inside the detected skin region during the mapping process, the mapping weights of M_{Cb_i} and M_{Cr_i} are calculated using these differences as follows:

$$\begin{aligned} M_{\mathrm{Cb}_i} &= |(\mathrm{Cb}_{S_p} - \mathrm{Cb}_i)/(S_{\mathrm{Cbmax}} - S_{\mathrm{Cbmin}})|^2, \\ M_{\mathrm{Cr}_i} &= |(\mathrm{Cr}_{S_p} - \mathrm{Cr}_i)/(S_{\mathrm{Crmax}} - S_{\mathrm{Crmin}})|^2, \end{aligned} \tag{15}$$

where S_{Cbmax}, S_{Cbmin}, S_{Crmax}, and S_{Crmin} are the maximum and minimum values of Cb and Cr in the detected skin region, respectively. Thus, if the difference between the chromaticity of the original skin color and the chromaticity of the preferred skin color is small, a low weight is applied to the preferred skin color reproduction. Conversely, if the difference between the chromaticity of the original skin color and the chromaticity of the preferred skin color is large, a high weight is applied. As a result, a smooth skin color is reproduced inside the detected skin region. The results of the skin color reproduction of Y_o, Cb_o, and Cr_o are calculated as follows. The luminance value of each original skin color, Y_i, is used as the luminance value for the preferred skin color, Y_o:

$$\begin{aligned} Y_o &= Y_i, \\ \mathrm{Cb}_o &= \mathrm{Cb}_i + M_{\mathrm{Cb}_i}(\mathrm{Cb}_{S_p} - \mathrm{Cb}_i), \\ \mathrm{Cr}_o &= \mathrm{Cr}_i + M_{\mathrm{Cr}_i}(\mathrm{Cr}_{S_p} - \mathrm{Cr}_i). \end{aligned} \tag{16}$$

These processes are repeated for all the detected skin regions. Figure 7 shows the skin color reproduction toward the racial preferred skin color, where the black points indicate the preferred skin color, the green points indicate the original skin color, and the red points indicate the reproduced preferred skin color. Finally, the reproduced skin color is converted into RGB color space for displaying.

EXPERIMENTAL RESULT

For the experimental evaluation of the proposed algorithm, an observer's preference test was performed. The subjective evaluation test involved 45 observers, 15 females and 30 males, aged 24–34. The eyesight of the observers was either normal or corrected with glasses. The test was conducted using a Macbeth Judge II-S viewing booth, which supports a standard illuminant (D65) with 750 lx. As shown in Figure 8, the experiments used six printed images that included single or multiple races. Figures 9 and 10 show a comparison of the skin color reproduction results for the child and baby images including a single race. Figs. 9(a) and 10(a) show unnatural images due to an excessively scarlet skin color. Panels (b) and (c) of Figs. 9 and 10 show the reproduced images when using the methods of Kao et al. and Nachlieli et al., while the reproduced images when using the proposed method are shown in Figs. 9(d) and 10(d). Figure 11 shows a comparison of the skin color reproduction results for the volunteer image including multiple races. Fig. 11(a)

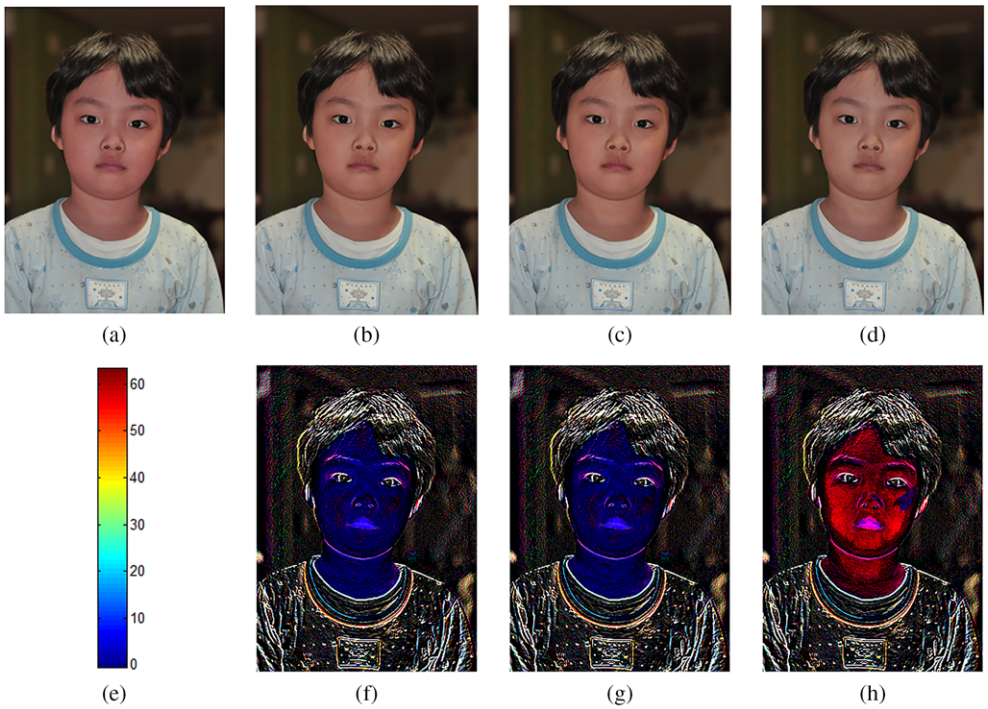

Figure 9. Original and resulting images with the proposed method using a single race child image: (a) original image; (b) resulting image using the method of Kao et al.; (c) resulting image using the method of Nachlieli et al.; (d) resulting image using the proposed method; (e) color bar for measuring color difference; (f) difference map between (a) and (b); (g) difference map between (a) and (c); (h) difference map between (a) and (d).

Figure 10. The original and resulting images by the proposed method using baby1 image of single race: (a) original image; (b) resulting image using the method of Kao et al.; (c) resulting image using the method of Nachlieli et al.; (d) resulting image using the proposed method; (e) color bar for measuring color difference; (f) difference map between (a) and (b); (g) difference map between (a) and (c); (h) difference map between (a) and (d).

shows that the input image had an excessively scarlet skin color, while Figs. 11(b)–(d) show the reproduced image when using conventional methods and the proposed method, respectively. For a better visual comparison, the difference maps between original and resulting images are calculated and scaled, as shown in panels (f)–(h) of Figs. 9–11.

Figure 11. The original and resulting images by the proposed method using the volunteer image of multiple races: (a) original image; (b) resulting image using the method of Kao et al.; (c) resulting image using the method of Nachlieli et al.; (d) resulting image using the proposed method; (e) color bar for measuring color difference; (f) difference map between (a) and (b); (g) difference map between (a) and (c); (h) difference map between (a) and (d).

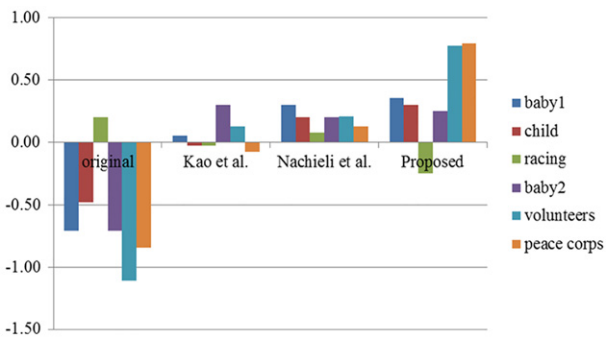

Figure 12. *Z*-scores for test images as a result of subjective evaluation.

The difference map represents the degree of skin color reproduction according to the color bar in panel (e) of Figs. 9–11. As shown, for the images with a single race, the skin color reproduction was similar when using the conventional and proposed methods. However, the proposed method output is a step ahead of the conventional methods when comparing the difference map. In the case of multiple races, the conventional method reproduces the skin colors of the different races toward a single preferred skin color, whereas using the proposed method, the skin colors of the different races are reproduced toward the respective race-selective preferred skin color.

The observers were then asked to rank each pair of reproduced images according to their preference, assigning 1 to the selected image and 0 to the rejected image. In the case of a tie, 0.5 was assigned to each image. The scores were then summed and converted to z-scores.[12] As shown in Figure 12, the z-scores for the proposed method were generally higher than those for the methods of Kao et al. and Nachlieli et al. Consequently, the proposed method achieved race-selective preferred skin color reproduction in images including single and multiple races.

CONCLUSION

This study proposed a race-selective preferred skin color reproduction method according to the user's preference. Skin regions are first detected using a combination of a focus map and a skin candidate map. The race is then classified by comparing the Euclidean distances between the average chromaticity of the detected skin region and the three chromaticities of the racial skin colors in the database. Based on this classification, the preferred skin color for each detected skin region is selected from a database of candidate racial preferred skin colors. Finally, the skin color is proportionally mapped toward the preferred skin color. Thus, in contrast to conventional methods, the proposed method is able to achieve preferred skin color reproduction for multiple races in a single image.

ACKNOWLEDGMENT

This work was supported by the National Research Foundation of Korea (NRF) grant funded by the Korea government (MSIP) (No. NRF-2013R1A2A2A01016105).

REFERENCES

[1] M. Tsukada, C. Funayama, and J. Tajima, "Automatic color preference correction for color reproduction," Proc. SPIE **4300**, 216–223 (2001).

[2] D. Sanger, T. Asada, H. Haneishi, and Y. Miyake, "Facial pattern detection and its preferred color reproduction," *Proc. IS&T/SID 2nd Color Imaging Conf.* (IS&T, Springfield, VA, 1994), pp. 149–153.

[3] S. N. Yendrikhovskij, F. J. J. Blommaert, and H. de Ridder, "Optimizing color reproduction of natural images," *Proc. IS&T/SID 6th Color Imaging Conf.* (IS&T, Springfield, VA, 1998), pp. 140–145.

[4] W. C. Kao, S. H. Wang, and C. C. Kao, "Color reproduction for digital imaging systems," IEEE Int. Symp. Circuit Syst. **1–11**, 4599–4602 (2006).

[5] S. N. Yendrikhovskij, F. J. J. Blommaert, and H. de Ridder, "Color reproduction and the naturalness constraint," Color Res. Appl. **24**, 52–67 (1999).

[6] D. H. Kim, H. C. Do, and S. I. Chien, "Preferred skin color reproduction based on adaptive affine transform," IEEE Trans. Consum. Electron. **51**, 191–197 (2005).

[7] H. Nachlieli, R. Bergman, D. Greig, C. Staelin, B. Oicherman, G. Ruckenstein, and D. Shaked, "Skin-sensitive automatic color correction," HP Technical Report: HPL-2009-13, pp. 1–13, 2009.

[8] P. Peer and F. Solina, "An automatic human face detection method," *Proc. 4th Computer Vision Winter Workshop* (1999), pp. 122–130.

[9] D. Chai and K. Ngan, "Face segmentation using skin-color map in videophone applications," IEEE Trans. Circuits Syst. Video Technol. **9**, 551–564 (1999).

[10] N. Herodotou, K. N. Plataniotis, and A. N. Venetsanopoulos, "Automatic location and tracking of the facial region in color video sequences," Signal Process., Image Commun. **14**, 359–388 (1999).

[11] J. Morovic, *Color Gamut Mapping* (John Wiley & Sons, 2008), pp. 53–71.

[12] H. C. Do, J. Y. You, and S. I. Chien, "Skin color detection through estimation and conversion of illuminant color under various illuminations," IEEE Trans. Consum. Electron. **53**, 696–706 (2007).